Effect of Nano-Silica on the Mechanical and Transport Properties of Lightweight Concrete

Hongjian Du[a,*] Suhuan Du[b] and Xuemei Liu[c,*]

[a]*Department of Civil and Environmental Engineering, National University of Singapore, 117576 Singapore*

[b]*China Railway 15th Bureau Group Co., Ltd, Luoyang 471013, China.*

[c]*School of Civil Engineering and Built Environment, Queensland University of Technology, QLD 4001, Australia*

*Corresponding authors. Tel.: +61 7 3138 0686; fax: +61 7 3138 1170

E-mail addresses: ceedh@nus.edu.sg (H. Du), x51.liu@qut.edu.au (X, Liu)

ABSTRACT

This paper investigated the influence of nano-silica (NS) on the mechanical and transport properties of lightweight concrete (LWC). The resistance of LWC to water and chloride ions penetration was enhanced despite strength marginally increased. Water penetration depth, moisture sorptivity, chloride migration and diffusion coefficient was reduced by 23% and 49%, 23% and 10%, 5% and 0%, 22% and 12% compared to the two reference LWC mixes (pure cement and 60% slag blended cement), respectively with 1% NS. Such improvements were attributed to more compact microstructures because the micropore system was refined and the interface between aggregates and paste was enhanced.

Keywords: Durability; Interfacial Transition Zone; Microstructure; Lightweight Aggregate; Pozzolanic Reaction.

Highlights

- The effect of nano-silica on transport properties of LWC is firstly reported.
- Interfacial transition zone became more compact and denser with nano-silica.
- Nano-silica can increase compressive strength and lower porosity of LWC.
- Resistance to water and chloride ion were both improved at 1% nano-silica.
- Both pure cement and 60% slag cement LWC showed similar results.

1. Introduction

Portland cement, one of the largest commodities consumed globally, has great advantages to be cast to any desired shape, cheap and fire resisting. However, cement also has weakness like brittleness, volume instability and porous system. Recently, the tremendous potential of nanotechnology to improve the performance of traditional cement-based materials has drawn increasing efforts from researchers and engineers to explore the promising applications. The bulk engineering properties of cement composites might be able to be modified by using nano-particles such as higher strength and durability by nano-SiO_2 [1]. In addition, some smart properties which are desired for special purpose can be equipped for cement-based materials, for instance, self-cleaning and discoloration resistance by nano-TiO_2 to address air pollution problem [2], strain or damage sensing by carbon-based nano-materials in the area of structural health sensing [3,4], and higher ductility by carbon nanotube or nanofiber in the field of seismic resistance [5,6]. Among these nano-particles, nano-silica (NS) is the most used and studied [7-22].

Previous studies on the use of NS in cementitious materials show that NS can accelerate the cement hydration rate and its pozzolanic reaction can densify the microstructures (via turning calcium hydroxide into C-S-H gel and nano-filling) [7-9]. Therefore, the strength is improved and the strength gain rate could be greatly increased for cement mixture with high amount of pozzolanic materials. More recently, the durability properties for concrete with NS have also been documented. Quercia et al. [19] examined the influence of 3.8% colloidal NS on the durability performances of self-compacting concrete (SCC) and found that the pores are finer and less connected. In addition, the paste-aggregate interface is also modified and more tortuous for harmful agents. Therefore, the water resistance under pressure, chloride diffusion and

migration coefficient can be reduced by 88.5%, 63.1% and 63.6%, respectively. Du et al. [23] reported the transport-properties related durability of normal-strength concrete added with powdered NS at dosage of 0.3 and 0.9%. Incorporating NS, the calcium hydroxide was rapidly consumed and at the same time paste pore systems were clearly refined, even at small NS addition of 0.3%. In addition to the reduction in water penetration depth and chloride migration and diffusion, the rate of water absorption was also much reduced, attributed to the less connected pores. Furthermore, some recent studies [20,21,24-26] explored the application of NS in high performance cementitious composites (HPCC). It is generally consistently reported that there exists a critical NS content beyond which the HPCC quality could not be further enhanced due to the fact that more voids would be entrained in the system. Du and Pang [25] found that 1.5-2.0% colloidal NS could produce the best mechanical and durability performances.

Lightweight concrete (LWC) is a type of concrete with air-dry unit weight between 400 and 2000 kg/m^3. For structural LWC, the unit weight ranges 1400 and 2000 kg/m^3 compared to that of 2400 kg/m^3 for normal weight concrete [27-31]. With reduced self-weight, the buildings can have smaller cross-sectional structural components and thus more effective usable spaces. It was previously found that the ITZ thickness would decrease with higher absorption capacity of lightweight aggregate since less water can accumulate in the vicinity of the aggregate particle [32-34]. Beyond that, LWC with lightweight aggregates also has the advantage of internal curing which can prevent shrinkage cracking and reduce permeability [35]. Previous research [30,31] has shown that micro-silica (or silica fume) could obviously increase the LWC resistance against water and chloride-ion ingress. The bond at the paste-lightweight aggregate interface is improved because of both better packing (particles in micrometer level) and pozzolanic reaction (amorphous silica). Until now, no literature on the use of silica in nanometer scale in LWC is

available, to the best knowledge of authors. Thus, this study aims to investigate the influence of colloidal NS on LWC, with a focus on the durability properties. In addition, the effects of NS will be compared for LWC with pure cement and those with slag cement.

2. Materials and Methods

2.1 Materials

Expanded clay spheres were used as lightweight aggregate in this study, with particle size in the range of 4.75 and 9.50 mm. The bulk density and dry particle density are 650 and 1200 kg/m^3, respectively. The water absorption is 8.4% at 1 h and 13.0% at 24 h, respectively. The total porosity of lightweight aggregate is 57.2%, 25.8% of which is open while the rest is closed.

Natural sand with a fineness modulus of 2.80 and specific gravity of 2.65 was used as fine aggregates. CEM I 52.5N cement and slag was used in this study, with chemical compositions shown in Table 1. The specific gravity for cement and slag is 3.25 and 2.90, respectively, as determined by Automatic Density Analyzer ULTRAPYC 1200e. Laser scattering particle size analyzer, Malvern Mastersizer was used to determine the particle size distribution (PSD) of cement and slag. It was assumed that the irregular shape of cement and slag particles as sphere to calculated the surface area and size distribution. Cement and slag were dissolved in acetone and sonicated in ultrasonic bath for 2 minutes to achieve uniform dispersion. PSD for natural sand was determined by sieve analysis and shown in Fig. 1, together with cement and slag. The morphology of the slag is shown in Fig. 2, as observed by scanning electron microscope (SEM).

Colloidal nano-silica[1] used in this study contains 40% solids and has a density of 1.3 g/mL. The surface area of nano-silica is 220 m^2/g (provided by the product supplier) and correspondingly the average particle size is 12.4 nm. Fig. 3 shows the dispersion and morphology of mono-sized nano-silica particles in the as-received suspension, using a JEOL JEM2010 TEM at an operating acceleration voltage of 100 kV. Polycarboxylate-based superplasticizer was used to control the workability for LWC mixtures. It is commonly recognized that colloidal NS can achieve better dispersion than powdered NS and thus yielding better packing density (or lower porosity in another word) and better performances [10,11]. At the same time, the risk assessment for powdered NS is more severe compared to colloidal NS, which may cause unfriendly working conditions and heavy personal protective equipments for researchers. Thus, colloidal NS was used in this study, although its price is higher.

2.2 Mix proportions and casting

Table 2 summarizes the mix proportions for LWC with NS. Mix proportion for the reference LWC-C0 was modified based on a normal weight concrete mixture (selected according to ACI 211.1, based on the raw materials used), by replacing the normal-weight coarse aggregates by lightweight aggregates at the equivalent volume. Colloidal NS was added into the reference LWC at 1% and 2% by weight of the cement, respectively, as recommended by previous work [25]. At the same time, 60% of the cement was substituted by slag by weight in the other reference LWC-S0. Because slag has a slightly lower specific density, sand content was reduced correspondingly to maintain a unit volume, as shown in Table 2. Similarly, 1% and 2% NS was added into this reference LWC. The water-to-cementitious (*w/cm*) ratio was kept as 0.42 for all

[1] LUDOX® HS-40 colloidal silica, W.R. Grace & Co.-Conn.

the concrete mixtures, for a target 28-day strength of 40 MPa, as suggested by ACI 211.1. It is noted that the water content in the NS aqueous suspension was calculated into the *w/cm* ratio. SP amount was adjusted to maintain the slump at 100 ±25 mm for each LWC mix, for the application of beams, reinforced walls or building columns as recommended by ACI 211.1.

Prior to pouring into concrete mixer, lightweight aggregates were oven-dried for 24 hours and cooled down to room temperature. Sand was poured and mixed with lightweight aggregates for 1 minute, following by adding cement (or slag cement). All the dry materials were mixed for 1 minute before water was added. Extra water was added with a calculated amount based on the 1-h water absorption by lightweight aggregates. For colloidal NS incorporated mix, NS was first dissolved in the mixing water and hand stirred for 1 minute. After adding water, the concrete mixtures were mixed for 3 minutes and SP was added to achieve the desired workability. Finally, the specimens were compacted on a vibration table. After that, the specimens were covered with a plastic sheet, until the next day. All the specimens were cured in fog room (100% RH, 30 ˚C) for 7 days and transferred to store in the laboratory air (80-85% RH, 30 ±3 ˚C), until the specified testing age.

2.3 Test methods and specimens

For each LWC mix, the test specimens and standard methods were summarized in Table 3. Compressive strength was determined at 1, 7 and 28 days. For all the other tests, preparation work was carried out at the age of 28 days. The water accessible porosity (φ, %) is determined as:

$$\varphi = \frac{m_A - m_O}{m_A - m_W} \times 100 \quad (1)$$

where m_A and m_W refers to the weight of specimen in air and water respectively, m_O refers to the weight of specimen after 105 ˚C oven dry for 7 days.

To determine the water penetration depth into concrete, two cylindrical specimens were exposed to 0.75 MPa water pressure for 3 days. The bottom and side surfaces were coated with impermeable epoxy while the top surface was exposed to water. The average water frontier was measured from the exposure surface after splitting the fresh specimen.

The sorptivity is the rate of water absorption of unsaturated concrete. Specimens (at 28 days) were kept in a dessicator (80% RH, 50 ˚C) for 3 days, followed by 18 days conditioning in sealed containers. After that, the side surface was sealed by epoxy and the top surface was attached by a plastic sheet to avoid the contact with water. The mass increase (Δm) of the concrete specimen was measured at the initial stage (every 10 minutes in the first half hour, and hourly until 6 hours) and the secondary stage (daily reading up to 10 days). The sorptivity (s, $\times 10^{-4}$ mm/s$^{0.5}$) was calculated as the slope of the mass increase verse the square root of time (t):

$$s = \Delta m / t^{0.5} \tag{2}$$

In this study, the specimens were saturated in water under vacuum condition, which is reported as the most efficient technique [36]. The same procedure was followed as the treatment method for specimens in rapid chloride penetration test (RCPT) to ensure the full saturation. A constant voltage of 30 V was applied to the specimen and the current (I_i) was measured for 12 hours, at a time step (Δt) of 5 minutes. The total charge passed (Q, Coulombs) was calculated as follows.

$$Q = \sum_{0}^{12h} I_i \cdot \Delta t \tag{3}$$

Compared to the voltage of 60 V specified by ASTM C 1202, the reduced voltage could lower the temperature rise during the test, to exclude the adverse effect of rising temperature [37].

Prior to rapid chloride migration (RCM) test, concrete specimens, with thickness (L) of 50 mm, were vacuum saturated in lime water. Chloride ions were forced to migrate along the applied electric field (U=30 V) through the specimen, for a duration (t) of 24 hours. After that, the average chloride penetration depth (d) was measured by spraying $AgNO_3$ (0.1 mol/L) on the freshly splitted specimens. With recorded temperatures before (T_1) and after (T_2) the RCM test, the chloride migration coefficient (D_{RCM}, $\times 10^{-12}$ m^2/s) could be calculated as:

$$D_{RCM} = \frac{0.0239(273+T)}{(U-2)t}\left(d - 0.0238\sqrt{\frac{(273+T)Ld}{(U-2)t}}\right), \quad T = (T_1+T_2)/2 \tag{4}$$

For chloride diffusion test, concrete specimens were coated with impermeable epoxy at all surface while only one cross section surface was uncoated for chloride ions to diffuse into. The specimens were immersed in sodium chloride solution for 84 days. Then the average acid-soluble chloride content (C) was determined for each layer of concrete at depth of 0-10 mm, 10-20 mm, 20-30 mm, 30-40 mm and 40-50 mm. The apparent chloride diffusion coefficient (D_a) and the surface chloride concentration (C_0) was determined by fitting the chloride profiles with the following equation,

$$C(x,t) = C_0\left[1 - erf\left(\frac{x}{2\sqrt{D_a t}}\right)\right] \tag{5}$$

where *erf()* is the error function.

SEM (Hitachi-4300) was employed to examine the influence of NS on the LWC microstructures. Samples were taken from the fractured surface after the compressive strength

test. They were dried in a vacuum oven at 40 ˚C until no weight loss can be recorded before SEM observation. Isothermal calorimetry was performed on triplicate paste samples by using an eight-channel microcalorimeter (TAM AIR). Shimadzu XRD-6000 diffractometer was employed to qualitatively determine the influence of NS on the chemical composition of the hydrated production. The XRD scan was between 10˚ and 35˚ with a speed of 0.5˚/min.

3. Results and Discussion

3.1 Hydration

Calorimetric test was conducted for cement paste with the same *w/cm* ratio to probe the influence of NS on the cement hydration, as shown in Fig. 4. For both pure cement and slag cement pastes, the peak rate was obviously increased with more colloidal NS which provides more nucleation sites. Also, the time to reach the peak hydration rate is also shortened, particularly for the second peak in Fig. 4(c), which represents the hydration of aluminum phase in slag. It is also noted that the addition of 2% NS did not further increase the total heat, in comparison to 1% NS addition at 72 h for slag cement paste. The slag activation was caused by the calcium hydroxide, which is a hydration product during the first peak. With the added NS, calcium hydroxide could be consumed by the pozzolanic reaction. Thus, there will be less to activate the slag, resulting in no further increase in the total heat. Meanwhile, an obvious increase in the total heat was found for pure cement paste from 1% to 2% NS addition. At the fresh state of the paste with NS, the ultra-fine silica particle can provide additional nucleation sites for precipitation of the cement hydration products. Previous literature has well documented that NS can accelerate the hydration

of cement or blended cement [10,17,18,21,25,26]. The results obtained in this study match with this general conclusion.

XRD patterns were shown in Fig. 5, for cement, slag, slag cement paste with 0%, 1% and 2% NS. Compared to the slag cement paste, the addition of NS could reduce the peak intensity for Portlandite, in a qualitative way, indicating that the Portlandite was consumed by the addition of nano silica.

3.2 Compressive strength

The compressive strengths of LWC (with average and range of the results) with different NS content at various ages are shown in Fig. 6. For pure cement LWC, compressive strength continues to increase with higher NS content at each test age. At the first day, an increase of 7.7% and 13.3% was noticed for 1% and 2% NS addition, respectively. However, this strength improvement was lowered to be 2.6% and 5.6% at 28-day, indicating that the NS benefits might fade with longer curing time. For slag cement LWC, 1% and 2% addition of NS could help increase 12.6% and 9.7% compressive strength on the first day. At 28 days, the improvement became marginal for 1% NS and 2% NS even slightly reduced the LWC strength. Overall, the LWC strength was noticeably improved at early age (within 7 days) and the enhancement was weak at a longer term. Such phenomenon for LWC is similar to what had been observed for the normal weight concrete [21].

At the early age, the use of NS can have two fold benefits to concrete, in both physical and chemical means. In addition to the cement acceleration effect, NS, similar as silica fume, can increase the packing density by filling the voids between cement grains and particularly the interface between the paste and aggregate. As a result, the cement hydration products can be

more compact and homogenous at the early age. With longer curing time, the unhydrated cement grains continue to hydrate for all the LWCs, especially for the two reference mixes in which more cement was unhydrated at the earlier age (both of which had the lowest total hydration heat). Thus, the relative strength increase for NS incorporated LWCs was lower at 28 days than those reference mixes, as described above. Furthermore, it is found that the slag cement LWCs are slightly lower in compressive strength than pure cement LWCs, indicating that the slag used in this study has a reactivity smaller than 1, as at 60% cement substitution. The marginal strength reduction in 2% NS slag cement LWC was possibly because NS could also compete for CH with slag for the pozzolanic reaction.

In LWC, the porous aggregate might be the weakest phase in LWC which is different from normal weight concrete in which the interface determines the strength. The fracture resistance of lightweight aggregate is not altered by the inclusion of NS despite the interface is improved. Therefore, the increase in the ultimate strength is marginal for LWC.

3.3 Water accessible porosity

Fig. 7 shows the influence of colloidal NS on the average water accessible porosity for pure cement and slag cement LWC (maximum and minimum test results are also plotted). The addition of NS seems to decrease the porosity at 1% dosage, for both reference LWCs. However, the porosity of LWC at 2% NS slightly increased than 1% NS LWC, more obvious for slag cement LWC. The results are consistent with the compressive strength. It is common knowledge that the mechanical strength of concrete is inversely proportional to its porosity. Compared to pure cement LWCs, the overall higher porosities for slag cement LWCs match the lower compressive strengths. The reduced porosity at 1% NS addition should be caused by the better

packing of solids and the pozzolanic reaction of NS which both contribute to more compact and homogeneous microstructures, particularly at the interface between paste and lightweight aggregates. Another non-ignorable fact is that the viscosity of NS incorporated paste would be increased due to less lubricating water is available in such pastes. As a result, the air content in the fresh concrete mixtures was higher compared to the reference mixture. When the densifying effect of NS is not sufficient to compensate the increase in air content, the porosity of hardened concrete might be increased, as reported for the 2% NS adding LWCs. Such impact of NS on LWC was similar to its impact on normal weight concrete [21,23]. Rong et al. [26] found that the change in the porosity is actually very marginal despite reduction was noticed up to 3% NS addition. Quercia et al. [19] also reported that the porosity was slightly altered by 3.8% NS. On the other hand, most of the previous literature states that the pore systems were refined by the use of NS.

Previous literature [38] has found some specific relationship between the water accessible porosity and the transport properties related durability performances of concrete including LWC. General speaking, the transport of water and ions in concrete could be either partially blocked or hindered if the water accessible porosity is reduced because the connected channels are lesser.

3.4 Water penetration depth

The influence of colloidal NS on the water penetration depth of pure cement and slag cement LWCs is plotted in Fig. 8, at 28 days. The average penetration depth was 8.67 mm and 5.97 mm for pure cement and slag cement LWC respectively. In contrast to compressive strength and water accessible porosity, slag cement LWC has higher resistance to water penetration under pressure than pure cement LWC. This is possibly due to the fact that other factors also affect the

water permeability besides the total porosity, for example, pore size distribution and the connectivity of pores. In this case, it is assumed that the slag cement LWC have a finer pore system due to the pozzolanic reaction of slag. Regarding the influence of colloidal NS on the water penetration depth, 1% dosage could obviously reduce the permeability while 2% dosage appears to have less noticed benefits, particularly for slag cement LWC. The reducing effect on water permeability originates from the filler effect of NS in voids between solids, same as its influence on porosity. In addition, the pozzolanic reaction of NS can turn CH to C-S-H gel, which could fill the voids and thus further densify the microstructures of paste. The results in this study agree with previous findings on normal weight concrete incorporating NS [19,23].

3.5 Water sorptivity

Sorptivity, at both initial and secondary absorption stages, for pure cement and slag cement LWCs are displayed in Fig. 9. It is clear that the sorptivity of pure cement LWC was continuously reduced with more NS addition, for both initial and secondary absorption stage. This is slightly different from the change in water accessible porosity and water penetration, which both exhibited the lowest value at 1% NS. A reduction of 35% and 32% was found for initial and secondary sorptivity, at NS dosage of 2%. For slag cement LWC, initial and secondary sorptivity decreases to be 73% and 83% at 1% NS incorporation. However, the relative ratio becomes to be 87% and 121% for initial and secondary sorptivity, respectively, at 2% NS dosage. This is consistent with the water penetration and compressive strength, might be caused by the hindered slag activation by the addition of 2% NS, as discussed in Section 3.1. Water sorptivity is a measure of water uptake rate into unsaturated mortar, and mainly governed by the pore structure like pore size, connectivity and tortuosity. At the same time, the

microstructures at the interfacial transition zone (ITZ) between LWA and cement paste were more compact by the use of NS, as clearly seen from Fig. 10. The above described results are in consistence with the change in water accessible porosity due to the addition of colloidal NS. Some recent research also finds the water sorptivity of normal-weight cement paste could be reduced by the addition of silica nano-particles [39], but to a smaller extent than that of LWC in this study.

3.6 RCPT and RCM tests

The results of RCPT and RCM test for LWCs are shown in Fig. 11. It is noted that the resistance of LWCs to chloride ion penetration under externally applied electric fields are improved, regardless of pure cement or slag cement. RCPT actually measures the electrical conductivity of concrete instead of its real permeability against chloride-ion. Thus, RCPT result is heavily affected by the concentration of ions (Ca^{2+}, OH^-, Na^+, K^+, etc.) in the pore solution, besides the pore system [40]. This is verified by the much lower RCPT result for slag cement LWCs than pure cement LWCs since slag would consume calcium hydroxide during its pozzolanic reaction. As mentioned in the preceding sections, the pore structure of LWC concrete would be refined by the use of NS (owning to both nano-filler effect and pozzolanic reaction), thus the pathway for ions would become more tortuous or partially blocked. On the other hand, the reduction of $Ca(OH)_2$ content also help increase the electrical resistance since less number of ions are available in the pore solution. Furthermore, it is surprising to see the 2% NS incorporated slag cement LWC shows the lowest RCPT result, only 66% of the reference mix. Considering this mix has larger porosity, we can assume that it is the depletion of $Ca(OH)_2$ and alkalis in the pore solution that contribute to an even larger reduction in this RCPT result.

The RCM results almost show the same trend as RCPT, that is, chloride-ion is less permeable to LWC with the use of colloidal NS. This reduction is more obvious for slag cement LWCs. With 2% NS, the chloride migration coefficient could be lowered as much as 36% for slag cement LWC, in comparison to a 4% reduction for pure cement LWC at the same amount. The higher aluminum content in slag could decrease the chloride ion mobility since its hydration products (C-A-H, C-S-H and C-A-S-H) have higher binding capacity [41-43]. Since the added NS can accelerate the cement hydration and slag pozzolanic reaction, products in the paste might prevent the chloride ions from migration under the externally applied electric field.

3.7 Chloride diffusivity

The chloride content profiles along the diffusion direction are plotted in Fig. 12(a), in which the best-fitted curve is also included for each LWC mix. Fig. 12(b) shows the chloride diffusion coefficient for both pure cement and slag cement LWCs containing colloidal NS. Slag cement LWC has clearly lower diffusion coefficient because of the refined pore system by pozzolanic reaction, as well as the higher chloride binding capacity, same as discussed in the previous section. The incorporation of NS could continuously decrease the chloride diffusion coefficient up to 2% in this study. A reduction of 20% in the diffusion coefficient could be achieved for both pure cement and slag cement LWCs. The reduced porosity of concrete (or the more compact microstructures) as well as the refined pore system leads to this higher resistance to chloride diffusion. Compared to RCPT and RCM tests which are both accelerating measurements by applying electrical field to force chloride ions to migrate into concrete specimen, it takes 84 days for the samples to complete the chloride diffusion test. During this period, further hydration and

pozzolanic reaction could continue to occur, manifesting the benefits of adding NS on the resistance to chloride ingress, particularly for the pure cement LWC incorporating 1% NS.

Also, it is noted that the transport of chloride ions (results from RCPT, RCM and diffusion) was less affected by the addition of NS, compared to the reduction in water transport, particularly at 1% NS addition. The highest improvement in resistance against chloride ion ingress occurred at 2% NS for LWC, indicating that chloride transport was hindered even the water porosity would be higher at 2% NS dosage. This might be due to the higher chloride binding capability of the formed C-S-H gel from pozzolanic reaction [41-43].

4. Conclusion

The influence of colloidal nano-silica in lightweight concrete was experimentally investigated at an adding dosage of 1% and 2%. The following conclusions can be drawn:

1) Early age strength could be improved by adding silica nano-particles for LWC owning to the higher cement hydration rate. However, such benefit on strength became weakened with extended curing time. For 2% NS added slag cement LWC, the strength was slightly decreased because available calcium hydroxide is less due to the consumption by amorphous silica. This reduction was not found for pure cement LWC with 2% NS.
2) In accordance with the compressive strength, water accessible porosity was also decreased with the addition of NS because of denser microstructures, resulted by the nano-filler effect and pozzolanic reaction. Beyond 1% addition, the porosity was slightly increased because more air voids could have been entrapped into the concrete mixture during mixing.

3) Both water penetration and sorptivity were reduced with the addition of nano-silica up to 2% for pure cement LWC. The transport of water matches with the porosity except the sorptivity for the pure cement LWC with 2% NS. An optimum content of 1% NS was found for slag cement LWC to achieve highest resistance to water penetration.
4) Both accelerated and non-accelerated tests indicate that higher resistance against chloride ion penetration was obtained by using nano-silica. Continuous improvement was observed with the increased NS content up to 2%, for both pure cement and slag cement LWC.

Acknowledgements

Ms. Li Wei and Mr. Ang Boo Ong are gratefully acknowledged for their great help with the materials characterization in this study, including paste hydration.

References

[1] K. Sobolev, M. Ferrara, How nanotechnology can change the concrete world – Part 1, Am. Ceram. Soc. Bull. 84 (2005) 16-20.
[2] P. Krishnan, M.H. Zhang, Y. Cheng, D.T. Riang, L.E. Yu, Photocatalytic degradation of SO_2 using TiO_2-containing silicate as a building coating material, Constr. Build. Mater. 43 (2013) 197-202.
[3] J.L. Le, H. Du, S.D. Pang, Use of 2-D Graphene Nanoplatelets (GNP) in cement composites for structural health evaluation, Compos. B. 67 (2014) 555-563.
[4] H. Du, S.T. Quek, S.D. Pang, Smart multifunctional cement mortar containing graphite nanoplatelet, in: J.P. Lynch, C.B. Yun, K.W. Wang (Eds.), Sensors and Smart Structures Technologies for Civil, Mechanical, and Aerospace System, San Diego, 2013. doi: 10.1117/12.2009005
[5] M.S. Konsta-Gdoutos, Z.S. Metaxa, S.P. Shah, Highly dispersed carbon nanotube reinforced cement based materials, Cem. Concr. Res. 40 (2010) 1052-1059.
[6] Z.S. Metaxa, M.S. Konsta-Gdoutos, S.P. Shah, Carbon nanofiber cementitious composites: Effect of debulking procedure on dispersion and reinforcing efficiency, Cem. Concr. Compos. 36 (2013) 25-32.

[7] T. Ji, Preliminary study on the water permeability and microstructure of concrete incorporating nano-SiO_2, Cem. Concr. Res. 35 (2005) 1943-1947.
[8] G. Li, Properties of high-volume fly ash concrete incorporating nano-SiO_2, Cem. Concr. Res. 34 (2004) 1043-1049.
[9] H.Li, H.G. Xiao, J. Yuan, J.P. Ou, Microstructure of cement mortar with nano-particles, Compos. B. 35 (2004) 185-189.
[10] T. Oertel, F. Hutter, R. Tanzer, U. Helbig, G. Sextl, Primary particle size and agglomerate size effects of amorphous silica in ultra-high performance concrete, Cem. Concr. Compos. 37 (2013) 61-67.
[11] T. Oertel, U. Helbig, F. Hutter, H. Kletti, G. Sextl, Influence of amorphous silica on the hydration in ultra-high performance concrete, Cem. Concr. Res. 58 (2014) 121-130.
[12] J.J. Gaitero, I. Campillo, A. Guerrero, Reduction of the calcium leaching rate of cement paste by addition of silica nanoparticles, Cem. Concr. Res. 38 (2008) 1112-1118.
[13] S. Kawashima, P. Hou, D. Corr, S.P. Shah, Modification of cement-based materials with nanoparticles, Cem. Concr. Compos. 36 (2012) 8-15.
[14] P. Hou, S. Kawashima, D. Kong, D.J. Corr, J. Qian, S.P. Shah, Modification effects of colloidal nanoSiO_2 on cement hydration and its gel porosity, Compos. B. 35 (2013) 12-22.
[15] P. Hou, S. Kawashima, K. Wang, D. Corr, J. Qian, S.P. Shah, Effects of colloidal nanosilica on rheological and mechanical properties of fly ash-cement mortar, Cem. Concr. Compos. 35 (2013) 12-22.
[16] D. Kong, X. Xu, W. Sun, H. Zhang, Y. Yang, S.P. Shah, Influence of nano-silica agglomeration on microstructure and properties of the hardened cement-based materials, Constr. Build. Mater. 37 (2012) 707-715.
[17] M.H. Zhang, J. Islam, S. Peethamparan, Use of nano-silica to increase early strength and reduce setting time of concretes with high volumes of slag, Cem. Concr. Compos. 34 (2012) 650-662.
[18] M.H. Zhang, J. Islam, Use of nano-silica to reduce setting time and increase early strength of concretes with high volumes of fly ash or slag, Constr. Build. Mater. 29 (2012) 573-580.
[19] C. Quercia, P. Spiesz, G. Husken, H.J.H. Brouwers, SCC modification by use of amorphous nano-silica, Cem. Concr. Compos. 45 (2014) 69-81.
[20] R. Yu, P. Tang, P. Spiesz, H.J.H. Brouwers, A study of multiple effects of nano-silica and hybrid fibres on the properties of Ultra-High Performance Fibre Reinforced Concrete (UHPFRC) incorporating waste bottom ash (WBA), Constr. Build. Mater. 60 (2014) 98-110.
[21] R. Yu, P. Spiesz, H.J.H. Brouwers, Effect of nano-silica on the hydration and microstructure development of Ultra-High Performance Concrete (UHPC) with a low binder amount, Constr. Build. Mater. 65 (2014) 140-150.
[22] S. Haruehansapong, T. Pulngern, S. Chucheepsakul, Effect of the particle size of nanosilica on the compressive strength and the optimum replacement content of cement mortar containing nano-SiO_2, Constr. Build. Mater. 50 (2014) 471-477.
[23] H. Du, S. Du, X. Liu, Durability performances of concrete with nano-silica, Constr. Build. Mater. 73 (2014) 705-712.
[24] R. Yu, P. Spiesz, H.J.H. Brouwers, Development of an eco-friendly Ultra-High Performance Concrete (UHPC) with efficient cement and mineral admixture uses, Cem. Concr. Compos. 55 (2015) 383-394.

[25] H. Du, S.D. Pang, Effect of colloidal nano-silica on the mechanical and durability performances of mortar, Key Eng. Mater. 629 (2014) 443-448.
[26] Z. Rong, W. Sun, H. Xiao, G. Jiang, Effects of nano-SiO_2 particles on the mechanical and microstructural properties of ultra-high performance cementitious composites, Cem. Concr. Compos. 56 (2015) 25-31.
[27] ACI 213R-14, Guide for structural lightweight-aggregate concrete, American Concrete Institute, Farmington Hills, MI (2014).
[28] K.S. Chia, M. H. Zhang, Water permeability and chloride penetrability of high-strength lightweight aggregate concrete, Cem. Concr. Res. 32 (2002) 639-645.
[29] M.H. Zhang, O.E. Gjorv, Characteristics of lightweight aggregates for high-strength concrete, ACI Mater. J. 88 (1991) 150-158.
[30] X. Liu, K.S. Chia, M.H. Zhang, Development of lightweight concrete with high resistance to water and chloride-ion penetration, Cem. Concr. Compos. 32 (2012) 775-766.
[31] X. Liu, K.S. Chia, M.H. Zhang, Water absorption, permeability, and resistance to chloride-ion penetration of lightweight aggregate concrete, Constr. Build. Mater. 25 (2011) 335-343.
[32] M.H. Zhang, O.E. Gjorv, Penetration of cement paste into lightweight aggregate, Cem. Concr. Res. 22 (1992) 47-55.
[33] R. Wasserman, A. Bentur, Interfacial interactions in lightweight aggregate concretes and their influence on the concrete strength, Cem. Concr. Res. 18 (1996) 67-76.
[34] A. Elsharief, M.D. Cohen, J. Olek, Influence of lightweight aggregate on the microstructure and durability of mortar, Cem. Concr. Res. 35 (2005) 1368-1376.
[35] P. Lura, M. Wyrzykowski, C. Tang, E. Lehmann, Internal curing with lightweight aggregate produced from biomass-derived waste, Cem. Concr. Res. 59 (2014) 24-33.
[36] Q.L. Yu, P. Spiesz, H.J.H. Brouwers, Development of cement-based lightweight composites – Part 1: Mix design methodology and hardened properties, Cem. Concr. Compos. 44 (2013) 17-29.
[37] G.A. Julio-Betancourt, R.D. Hooton, Study of the Joule effect on rapid chloride permeability values and evaluation of related electrical properties of concretes, Cem. Concr. Res. 34 (2014) 1007-1015.
[38] X. Liu, H. Du, M.H. Zhang, A model to estimate the durability performance of both normal and light-weight concrete, Constr. Build. Mater. under review.
[39] P. Hou, X. Cheng, J. Qian, R. Zhang, W. Cao, S.P. Shah, Characteristics of surface-treatment of nnao-SiO_2 on the transport properties of hardened cement pastes with different water-to-cement ratios, Cem. Concr. Compos. 55 (2015) 26-33.
[40] C. Shi, Effect of mixing proportions of concrete on its electrical conductivity and the rapid chloride permeability test (AASHTO T277 and ASTM C1202) results, Cem. Concr. Res. 34 (2004) 537-545.
[41] H. Zibara, R.D. Hooton, M.D.A. Thomas, K. Stanish, Influence of the C/S and C/A ratio of hydration products on the chloride ion binding capacity of lime-SF and lime-MK mixtures, Cem. Concr. Res. 38 (2008) 422-426.
[42] M.D.A. Thomas, R.D. Hooton, A. Scott, H. Zibara, The effect of supplementary cementitious materials on chloride binding in hardened cement paste, Cem. Concr. Res. 42 (2012) 1-7.
[43] M. Otieno, H. Beushausen, M. Alexander, Effect of chemical composition of slag on chloride penetration resistance of concrete, Cem. Concr. Compos. 46 (2014) 56-64.

1

List of Tables and Figures

Table 1 Chemical compositions (% by mass) for cement and slag.

	SiO_2	Al_2O_3	Fe_2O_3	CaO	MgO	SO_3	Na_2O	K_2O
Cement	20.8	4.6	2.8	65.4	1.3	2.2	0.31	0.44
Slag	32.15	12.87	0.36	40.67	6.05	4.95	0.28	0.51

Table 2 Mix proportions and dry density for LWCs (*w/cm* = 0.42).

Mix No.	Content, kg/m^3							Density[a], kg/m^3	Density[b], kg/m^3
	Water	Cement	Slag	Sand	LWA*	NS[§]	SP[#]		
LWC-C0	180	430	—	1000	345	0	1	1990	1900
LWC-C1	174	430	—	1000	345	4.3	1.8	2025	1890
LWC-C2	167	430	—	1000	345	8.6	4.3	1990	1880
LWC-S1	180	172	258	975	345	0	1	1980	1855
LWC-S2	174	172	258	975	345	4.3	2	1990	1875
LWC-S2	167	172	258	975	345	8.6	4.1	1960	1845

*LWA: lightweight aggregate;

[§] NS: nano-silica, weight of solids;

[#] SP: superplasticizer; weight of aqueous suspension;

[a] Air-dry density;

[b] Oven-dry density.

Table 3 Test specimens and standard methods for each LWC mix.

Test	Number of specimens	Specimen	Standards
Compressive strength	3	Ø100×200 mm cylinder	ASTM C 109
Accessible water porosity	3	Ø100×50 mm slice	ASTM C 642
Water sorptivity	3	Ø100×50 mm slice	ASTM C 1585
Water penetration depth	2	Ø100×200 mm cylinder	BS EN 12390-8
RCPT	3	Ø100×50 mm slice	ASTM C 1202
RCM	3	Ø100×50 mm slice	NT Build 492
Chloride diffusion test	1	Ø100×100 mm slice	NT Build 443 & BS 1881-124

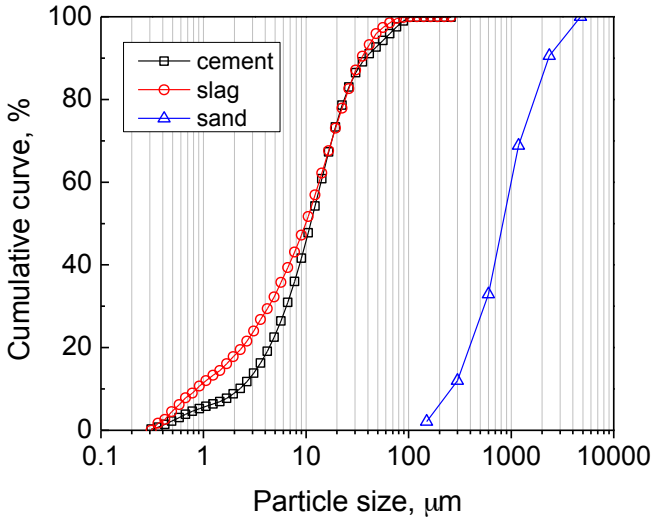

Fig. 1. Particle size distribution of raw materials.

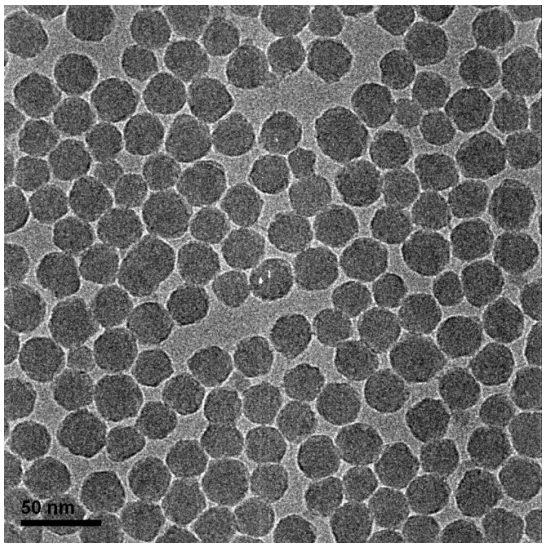

Fig. 2. TEM image of colloidal nano-silica used in this study.

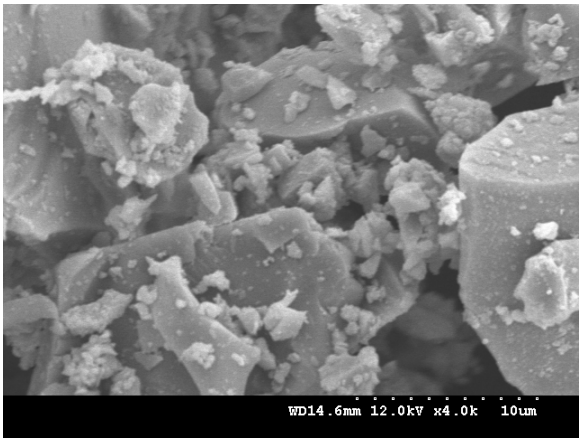

Fig. 3. SEM image of slag used in this study.

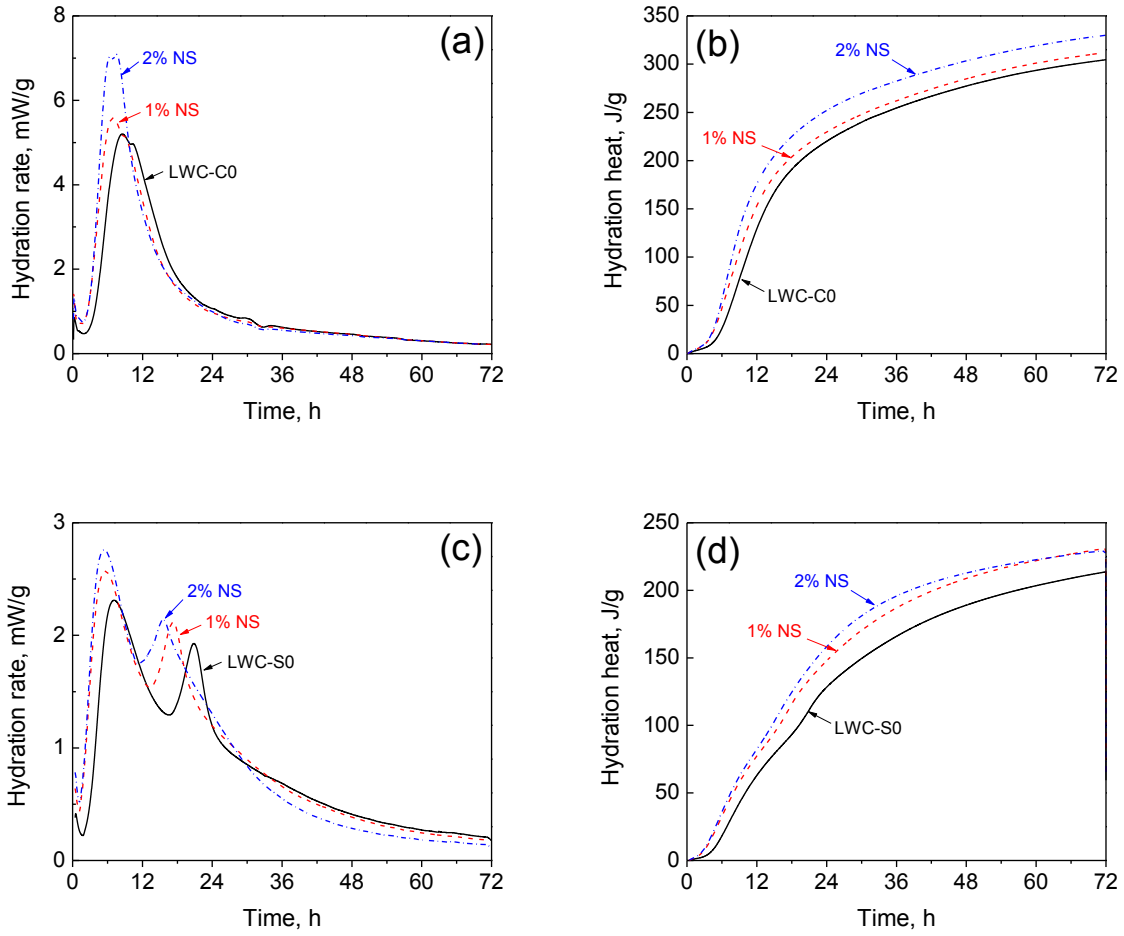

Fig. 4. Paste hydration results: (a) hydration rate and (b) total heat generated for NS incorporated pure cement paste, (c) hydration rate and (d) total heat generated for NS incorporated slag cement paste.

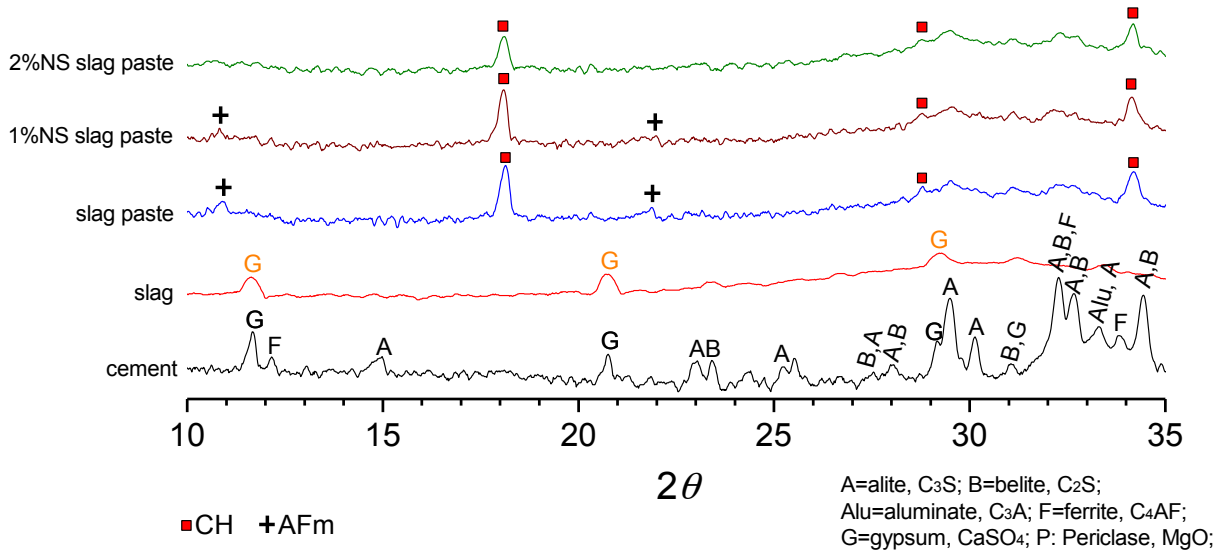

Fig. 5. XRD patterns for cement clinker and slag before casting, and slag cement pastes with 0, 1% and 2% NS at the age of 3 days.

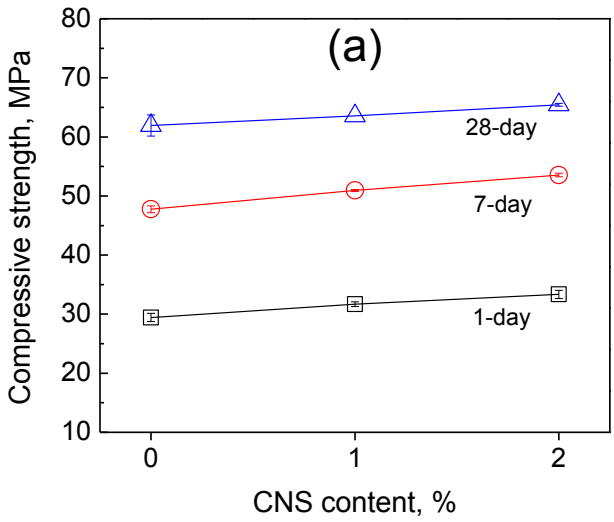

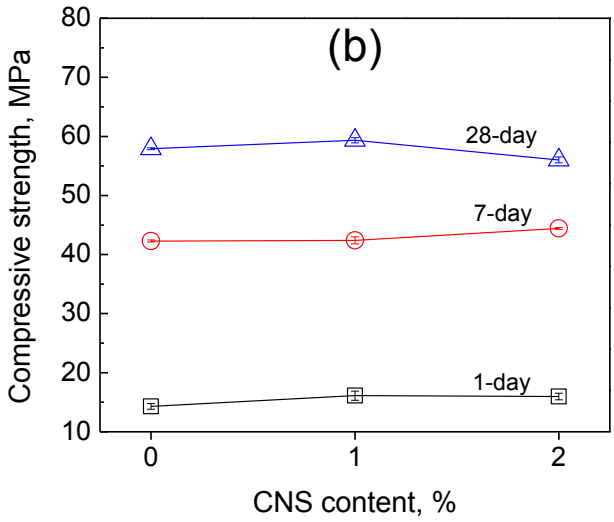

Fig. 6. Compressive strength of NS incorporated LWC with (a) plain cement and (b) slag cement.

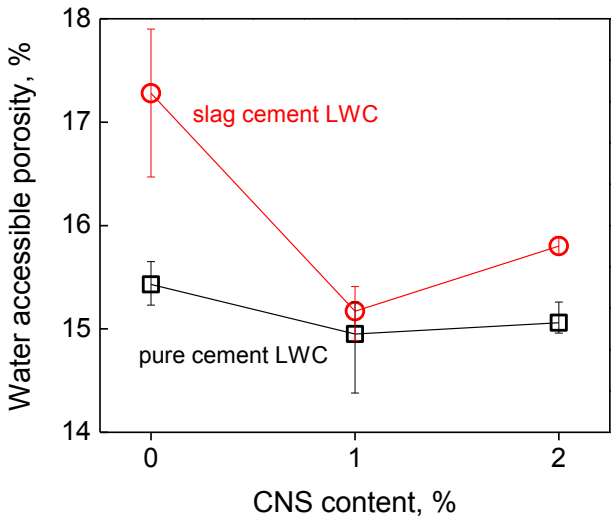

Fig. 7. Water accessible porosity of NS incorporated LWCs.

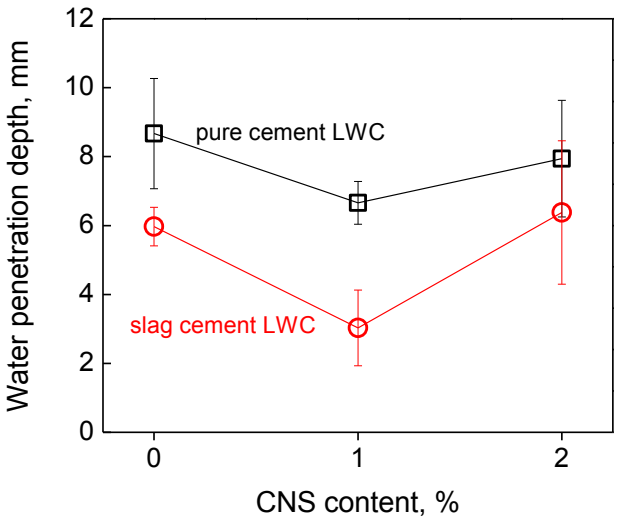

Fig. 8. Water penetration depth into NS incorporated LWCs.

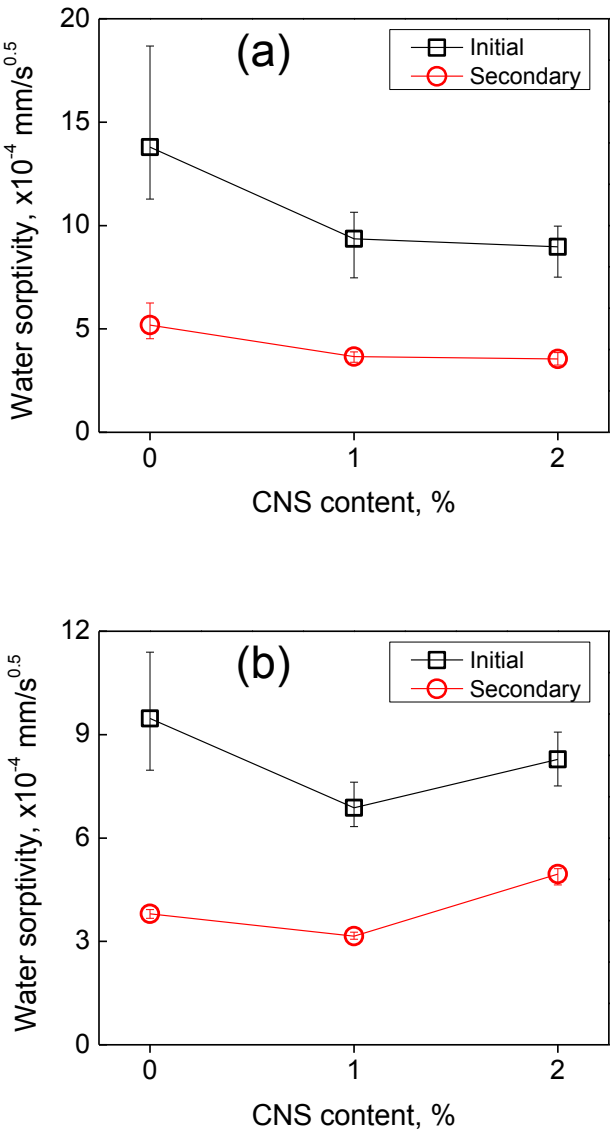

Fig. 9. Water sorptivity of NS incorporated LWCs with (a) pure cement and (b) slag cement.

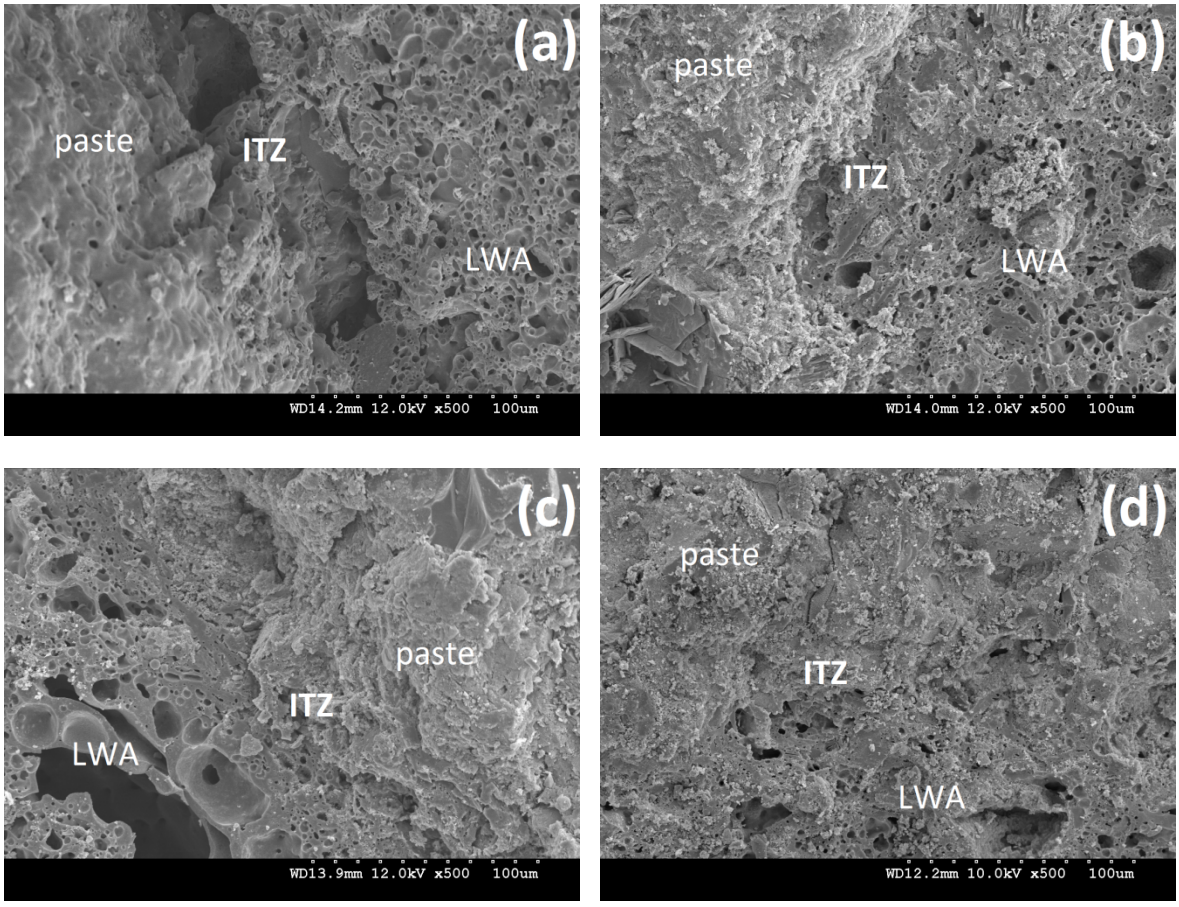

Fig. 10. Microstructures at ITZ for (a) pure cement LWC, (b) 1% NS added pure cement LWC, (c) slag cement LWC, and (d) 1% NS slag cement LWC.

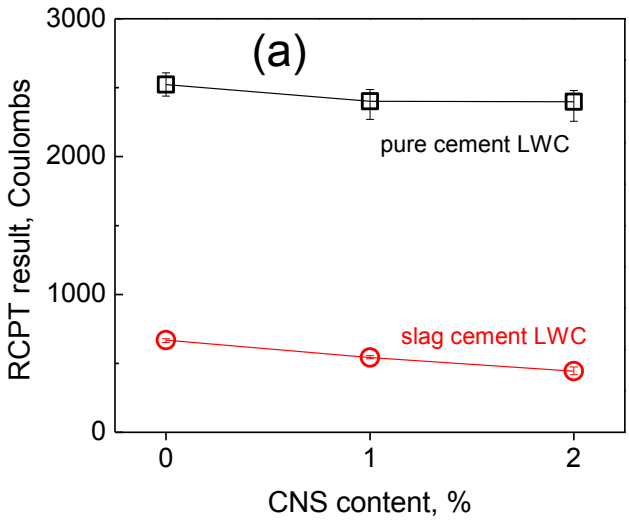

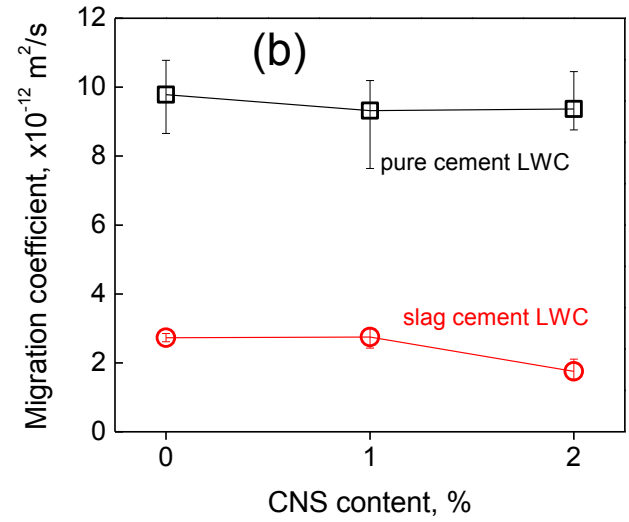

Fig. 11. (a) RCPT and (b) RCM testing results for NS incorporated LWCs.

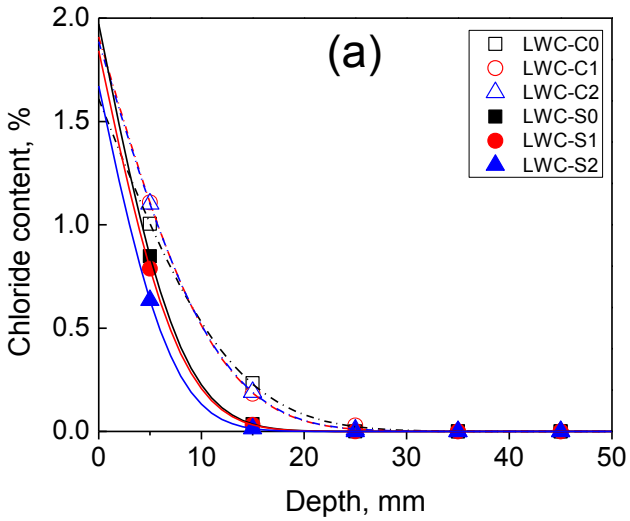

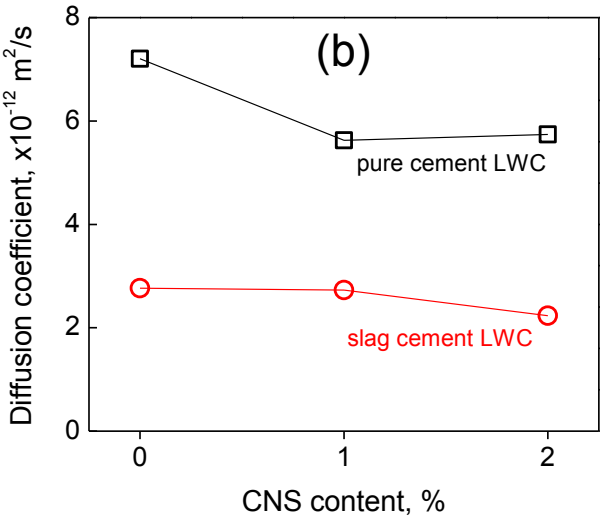

Fig. 12. (a) Chloride content profiles and best-fitted curves and (b) best-fitted diffusion coefficient into NS incorporated LWCs.